Polymer Journal, Vol. 28, No. 9, pp 769—779 (1996)

Super-Molecular Structures Controlling the Swelling Behavior of Regenerated Cellulose Membranes

Tomoko HONGO (née HIRASAKI), Chihiro YAMANE, Masatoshi SAITO, and Kunihiko OKAJIMA

Fundamental Research Laboratory for Natural & Synthetic Polymers, Asahi Chemical Industries Co., Ltd., 11-7 Hacchonawate, Takatsuki, Osaka 569, Japan

(Received February 15, 1996)

ABSTRACT: Swelling behavior of the regenerated cellulose membranes prepared from cellulose solutions dissolved in aqueous cuprammonium hydroxide and in dimethylacetamide/lithium chloride by various coagulation systems was discussed with special emphasis on crystal plane orientation and amorphous structures characterized by mechanical relaxations. Swelling anisotropy L_t to thickness direction of the membrane was observed without exception and was found to be categorized into three groups due to coagulation systems (acid, alkaline, and organic systems). Acid coagulation system was omitted from discussion because of discussion elsewhere. L_t was well correlated with crystallinity χ_c and its $(1\bar{1}0)$ plane orientation parameter $f_{\parallel(1\bar{1}0)}$, showing that larger those values give larger L_t. Larger L_t (hence, larger χ_c, or larger $f_{\parallel(1\bar{1}0)}$ in turn was confirmed to be related with higher T_{max} for α_2 and lower α_{H_2O}, β, and γ relaxations, and with larger $\tan\delta_{max}$ for all relaxations. These results lead to a conclusion that higher order molecular packing (stronger intermolecular hydrogen bonding) including crystalline part might accompany with the amorphous structure having more mobile local segmental motions during membrane formation studied here. Of these relaxations, β relaxation was confirmed to be composed of two mechanical relaxation mechanisms, one associated with out-of-phase local motion against $(1\bar{1}0)$ plane-like structure and the other associated with in-phase segmental motion. The swelling anisotropy was tentatively concluded as a phenomenon that arises from water penetration to more mobile parts, plasticizing molecular chains and integrating some of them along originally existed elementary crystals to the plane orientation direction according to $f_{\parallel(1\bar{1}0)}$, or simply rearranging the elementary crystals to the thickness direction, and of course water is retained between them.

KEY WORDS Swelling Anisotropy / Plane Orientation / Mechanical Relaxation / Regenerated Cellulose / Membrane Formation / Amorphous Structure

The relatively low dimensional stability of the regenerated cellulose shaped articles such as fibers and membranes due to their swelling behavior has been regarded one of problems to overcome since cotton exhibits higher tenacity and modulus in wet state than in dry state. Dimensional stability of polymers should be related to their morphology and super-molecular structure especially in their amorphous region because of the natural consequence that any structural change must start from the amorphous region if polymers are composed of crystalline and amorphous regions. In other words, the controlling of the morphology and super-molecular structure might lead to the shaped articles of polymers with good dimensional stability. One of examples is the dissolution of cellulose into aqueous (aq.) sodium hydroxide by breaking the intramolecular hydrogen bond to some extent and the resulting solution has been used for fabrication of fibers, demonstrated by authors.[1-6] One another example, also shown by authors,[7-9] is that nylon 66 can be fabricated into fiber and film having strong molecular interaction in amorphous region only controlling the terminal group balance. So far, Sakurada *et al.*[10] have proved that water molecules in so-called hydrocellulose, which was prepared by washing soda-cellulose derived from natural cellulose (Na-Cel I) to the alkali-free level, are retained in $(1\bar{1}0)$ plane by X-ray analysis. With small angle X-ray analysis on the dry and wet celluloses Hermans *et al.*[11] have detected the increase in scattering intensity of X-ray for the latter wet cellulose. Hayashi *et al.*[12] proposed by X-ray and IR analysis on the cellulose/potassium acetate adapt prepared by treating viscose rayon with concentrated aq. potassium acetate solution that molecular chains in amorphous region of the regenerated cellulose are not disordered but are integrated into some ordered plane-lattice structure ($(1\bar{1}0)$ plane). Manabe *et al.*[13] studied the mechanical relaxation behavior of regenerated cellulose in the temperature range of 280—600 K mostly at frequency of 110 Hz, and found three major relaxations α_3 (at 303—323 K), α_2 (at 413—563 K), and α_1 (at 558—578 K) after their terminology, attributing them as the cooperative motion of absorbed water and segments without hydrogen bondings, the micro-Brownian motion of segments with moderately developed hydrogen bondings (split into two absorptions depending on packing density) and the micro-Brownian motion of segment with strong hydrogen bondings. They also reported a relaxation α_{sh} seen at 388—473 K which was said to be only visible for the samples with higher crystallinity. In connection to the dimensional stability of cellulose against water, they demonstrated that water molecules penetrate into loosely packed molecular chains and act as plasticizer, causing all absorptions observed at dry state to appear at lower temperature side. Bradley *et al.*[14] reported 2 relaxations (β and γ from the higher temperature) at far lower temperature region for cellophane film seen at 240 K, 180 K, and assigned them as the local rotational motion of segment and the rotational motion of C_6 around C_5—C_6 axis in amorphous region, respectively. Takahashi[15,16] carried out X-ray analysis (both parallel and perpendicular directions to film) on dry viscose rayon films, prepared by coagulating and

regenerating the viscose solution cast on a glass plate with aq. sulfuric acid, and found that the degree of swelling of the films is higher for the films with higher degree in $(1\bar{1}0)$ plane orientation. He also considered that the plane orientation of $(1\bar{1}0)$ plane is caused by compression of film due to anisotropic dehydration to thickness direction during the acid coagulation process and the swollen water is selectively retained between $(1\bar{1}0)$ planes stabilized by hydrogen bonding. However, his consideration is unfortunately not always justified by other structural evidences, especially amorphous structural evidence. Authors[17] already demonstrated that the distribution of morphology (average pore size distribution) in the thickness direction of the regenerated cellulose membranes obtained from its cuprammonium hydroxide solution is largely categorized into three types (gradient structure (G-I), reverse gradient structure (G-II), homogeneous dense structure (HD)) depending on the pH or cation species of coagulants used. All these results give some essentials for possibility of controlling the super-molecular structure including morphology of cellulose. However, as is well known for polyamides in which molecular chains are basically bonded by hydrogen bondings like as cellulose, they exhibit the mechanical relaxations termed as β and γ below 0°C which are quite sensitive to water and are attributed to the segmental motion of water bonded to amide group including in part methylen moiety,[18-20] then one can easily imagine similar situation for cellulose. In fact a non-frequency dependent relaxation around -50°C for viscose rayon by forced longitudinal vibration at 8—80 Hz was reported by Dunell and Price.[21]

In this paper the swelling behavior of the regenerated cellulose membranes will be discussed in terms of super-molecular structure including morphology with emphasis on the nature of plane orientation and the mechanical molecular relaxation phenomena observed at low temperature. In this connect, mechanical relaxation mechanisms will be also briefly discussed.

EXPERIMENTAL

Cellulose Solutions

Two kinds of cellulose solutions were prepared by following procedures:

Cellulose/cuprammonium solution (Solution I): Cotton linter with the viscosity-average molecular weight $M_w = 1.7 \times 10^5$ was dissolved in aq. cuprammonium hydroxide solution according to the known procedure[22] at cellulose concentrations of 7, 8, and 10 wt%. M_w was estimated by using the equation $[\eta] = 3.85 \times 10^{-2} M_w^{0.76}$ established for cellulose/cadoxen system.[23]

Cellulose/DMAc-LiCl solution (Solution II): The above cotton linter was dissolved at cellulose concentration of 3 wt% in dimethylacetamide (DMAc) containing 8 wt% of lithium chloride (LiCl) according to the procedure described by Turbak *et al.*[24]

Preparation of the Regenerated Cellulose Membranes

Solution I was cast on a glass plate to give thickness of 250 μm, immersing gently into various coagulants (500 ml) for 1 min at 25°C, washed by water at 40°C for 1 min and regenerated by 2 wt% aq. sulfuric acid for 10 min, followed by washing with water. The resultant wet membranes were immersed into acetone sufficiently to exclude water, then placed between paper filter, followed by dried in air with a given dimension. Coagulants used are water, sodium hydroxide, sulfuric acid, sodium chloride, ammonium sulfate, and acetone with desired concentration in water, listed in Table I. All chemicals employed were guaranteed grade and supplied from Wako Pure Chemicals Co., Ltd., Japan. In another line of preparation, Solution II was cast on a glass plate to give thickness of 500 μm, immersing gently into acetone or toluene (500 ml) for 1 min at 25°C, washed by methanol. After substituting methanol by acetone the similar drying procedure described above was applied.

Swelling of the Cellulose Membranes

The dried cellulose membranes (cut into size *ca.* $2.0(=l_{1d}) \times 2.0(=l_{2d})$ cm and thickness of t_d μm) were dipped in to water at 25°C for 15 min and thickness (t_w) and length (l_{1w}, l_{2w}) were measured and the degree of swelling for the thickness (L_t) and longitudinal (L_l) directions, and the degrees of areal (A_s) and volumetric swelling (V_s) are defined as follows:

$$L_t = t_w/t_d \tag{1}$$

$$L_l = (l_{1w}/l_{1d} + l_{2w}/l_{2d})/2 \tag{2}$$

$$= l_{1w}/l_{1d} \tag{2'}$$

$$A_s = L_l^2 \tag{3}$$

$$V_s = L_t \times A_s \tag{4}$$

Note that significant longitudinal swelling anisotropy was not observed (that is, $l_{1w}/l_{1d} = l_{2w}/l_{2d}$).

Porosity and Water Permeability of the Wet Membranes

Porosity P_r of the wet membranes with area of 9.1 cm^2 cut out circularly was estimated by measuring its thickness L (cm) and its dried weight (that is, cellulose weight; W_d g) as follows:

$$P_r = 1 - W_d/9.1L\rho$$
(ρ is density of cellulose $= 1.561$ g cm^{-3}) (5)

X-Ray Diffraction Analysis

Orientation of crystal planes ($(1\bar{1}0)$ and (200)) was analyzed by irradiating both directions perpendicular to the cross section (that is, parallel to surface) and the surface area of the membranes by using a X-ray diffractometer (DH0002AM3X, Rigaku Denki, Japan). Diffraction intensities ($I_{\parallel(1\bar{1}0)}$, $I_{\perp(1\bar{1}0)}$) at $2\theta = 12°$, those ($I_{\parallel(110)}$, $I_{\perp(110)}$) at $2\theta = 20°$ and those ($I_{\parallel(200)}$, $I_{\perp(200)}$) at $2\theta = 21°$ were measured. Orientation factor $f_{\parallel(1\bar{1}0)}$ for $(1\bar{1}0)$ plane to the parallel direction to the membrane surface was evaluated in order to correct the possible difference in plane structure among membrane samples according to Takahashi[15,16] as follows:

$$f_{\parallel(1\bar{1}0)} = \{I_{\parallel(1\bar{1}0)}/(I_{\parallel(200)} + I_{\parallel(110)})/2\text{-}I_{\perp(1\bar{1}0)}/(I_{\perp(200)} + I_{\perp(110)})/2\}/\{I_{\parallel(1\bar{1}0)}/(I_{\parallel(200)} + I_{\parallel(110)}/2\} \tag{5}$$

$f_{\parallel(1\bar{1}0)}$ takes 0 (45° to thickness direction) to 1 (parallel to surface).

Crystallinity χ_c was estimated with regard to (200)

planes according to Segal's procedure[25] using the relation:

$$\chi_{c(200)} = 100\{I_{(200)} - I_{am}\}/I_{(200)} \quad (6)$$

Here, I_{am} means amorphous intensity at $2\theta = 16°$ and tends to be overestimated without correction based on a complete amorphous cellulose samples. For this purpose, a complete amorphous sample obtained from cellulose/aq calcium thyocyanete solution by acetone coagulation[26] and the peak intensity ratio $i_{(200)}/i_{am}$ was used as correction factor as shown in eq 7

$$\chi_{c(200)} = 100\{1 - (I_{am}/I_{(200)}) \times (i_{(200)}/i_{am})\} \quad (7)$$

Small angle X-ray diffraction measurement for a typical membrane (C10Na11) placed in a dried glass capillary and in a water containing capillary was made on a X-ray diffractometer (Rotor Flex RU-200PL, Rigaku Denki Co., Ltd., Japan) with transmission method by irradiating X-ray to the perpendicular and parallel directions against membrane.

Viscoelastic Analysis

The viscoelastic properties ($\tan\delta$–T, E'–T curves) for the membranes with size of $3 \times 40 \times 0.08$ mm were recorded on a viscoelastic spectrometer (Model SDM-5000, Seiko Densi, Co., Ltd., Japan) under the following conditions: Frequency, 10 Hz; heating rate, 10°C min^{-1}; measuring interval, 1°C min^{-1}; sample length, 20 mm; adding amplitude, 16 μm; initial charge to film, 115 g mm^{-2}; scanning of temperature, −150—350°C; if not specially indicated.

Cross Sectional Morphological Distribution

The wet membranes were freezed and their cracked cross section was subject to scanning electron microscopic observation (FE-SEM model S-800, Hitachi Seisakusyo Co., Ltd., Japan). According to the definition of the distribution of morphology in the thickness direction given in our previous paper,[15] membranes prepared were classified into G-I (gradient pore size distribution with larger pore on the surface side directly contacted with coagulant), G-II (reverse gradient pore size distribution), and HD (homogeneously dense morphology).

RESULTS AND DISCUSSION

Table I summarizes the morphological and the swelling parameters and the membrane preparation conditions of the membranes as well as the structural parameters determined by X-ray analysis, as will be explained below.

Figure 1 shows typical X-ray diffraction photographs and patterns of the membranes (a, C10Na11; b, C10Hs15; c, C07Ac30; d, D03T50) taken at different irradiating directions. Obviously, for the two membranes (C10Na11, C10Hs15), the $(1\bar{1}0)$ crystal plane appeared at $2\theta = 12°$ exhibits parallel orientation in general and the (200) plane at $2\theta = 21°$ is oriented to perpendicular direction. The other two membranes (C07Ac30, D03T50) do not show characteristic parallel $(1\bar{1}0)$ plane orientation and perpendicular (200) plane orientation, although some perpendicular orientation nature of $(1\bar{1}0)$ plane is seen for the former membrane. The parameter $f_{\parallel(1\bar{1}0)}$ describing the parallel crystalline plane orientation of $(1\bar{1}0)$ plane for the membranes are also listed in Table I with crystallinity χ_c, assuming that these parameters are also one of measures for the molecular orientation in amorphous region, as pointed out by Hayashi *et al.*[12] Note that the larger of $f_{\parallel(1\bar{1}0)}$ value denotes the higher ordering of hydrogen bonding in the thickness direction of the membrane.

Table I shows that porosity P_r widely deviates from 7 to 75% and seems to be lower for the membranes with HD morphology. Cellulose concentration is not a decisive factor controlling P_r but for a given solution/coagulation system the higher cellulose concentration seems to give smaller P_r. The crystallinity χ_c and $(1\bar{1}0)$ plane orientation $f_{\parallel(1\bar{1}0)}$ are lower for the membranes obtained by using organic coagulant system or using the cellulose solution dissolved in organic solvent system, of which membrane morphology is characterized by HD. The considerable swelling anisotropy to thickness direction for all membranes were observed and three parameters P_r, χ_c, and $f_{\parallel(1\bar{1}0)}$ are plotted against the swelling anisotropy parameter L_t in Figures 2a, b, and c. Numbers on Figure 2a denote χ_c. Figure 2a shows that on the whole L_t decreases with an increase in P_r, indicating that the reciprocal of P_r is one of the measures

Table I. Some morphological, structural and swelling parameters of the regenerated cellulose membranes and their preparation conditions

Sample[a]	Coagulant	Morphology	Porosity	Thickness	Crystallinity	$f_{\parallel(1\bar{1}0)}$	Swelling parameters		
		type	P_r/%	l_d/μm	χ_c/%		L_t	L_l	V_s
C10Na11	NaOH	HD	7.6	15.4	34.2	0.350	1.97	1.07	2.26
C10Hs15	H_2SO_4	G-II	22.0	32.9	42.0	0.520	1.99	1.08	2.32
C08Hs05	H_2SO_4	ditto	71.9	59.9	39.3	0.236	1.41	10.4	1.53
C08Hs10	H_2SO_4	ditto	31.2	39.9	38.1	0.463	1.65	1.07	1.90
C08Hs20	H_2SO_4	ditto	36.1	39.0	36.0	0.498	1.64	1.07	1.89
C08Na10	NaOH	HD	18.8	48.2	27.0	0.249	1.74	1.10	2.10
C08Nc10	NaCl	G-I	27.3	39.3	26.0	0.260	1.67	1.13	2.13
C08Ns10	$(NH_4)_2SO_4$	G-II	75.1	78.0	39.7	0.238	1.21	1.01	1.23
C07Ca10	$CaCl_2$	HD	16.0	15.9	21.2	0.175	1.71	1.08	1.99
C07Ac30	Acetone	HD	66.0	52.0	13.3	0.096	1.61	1.12	2.02
D03T50	Toluen	HD	18.8	7.9	5.5	0.094	1.58	1.03	1.68
D03Ac100	Acetone	HD	46.3	9.2	4.0	0.086	1.44	1.01	1.47

[a] First term C and D denote cuprammonium solution and DMAc/LiCl solution, first number means cellulose concentration, last number means coagulant concetration.

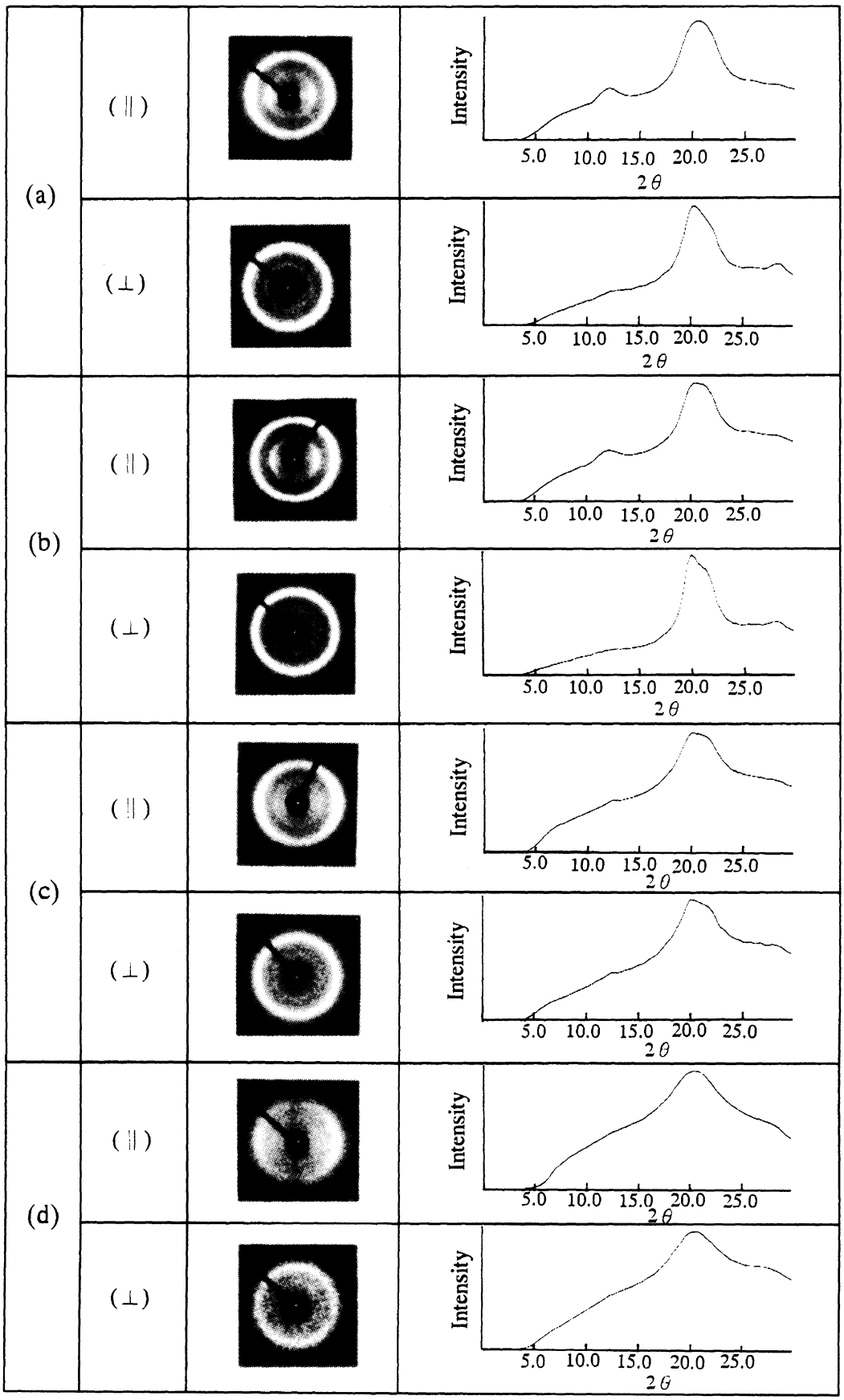

Figure 1. X-Ray diffraction micrographs and diffraction patterns of typical membranes taken at parallel (∥) and perpendicular (⊥) directions: (a), C10Na11; (b), C10Hs15; (c), C07Ac30; (d), D03T50.

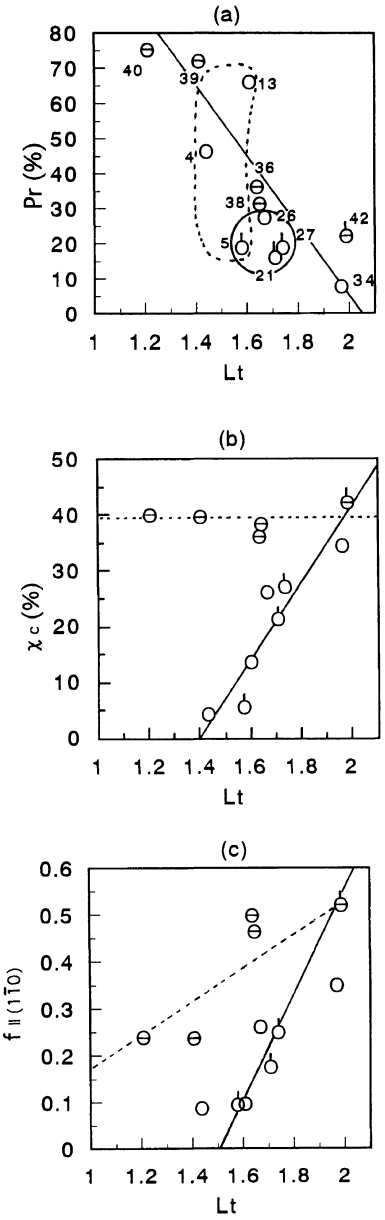

Figure 2. Dependence of swelling anisotropy parameter L_t on porosity P_r (a), crystallinity χ_c (b), and (1$\bar{1}$0) plane orientation parameter $f_{\parallel(1\bar{1}0)}$ (c): ⊖, membranes obtained by acid coagulation system; ○, membranes with almost constant P_r; ○, membranes obtained by other coagulation systems.

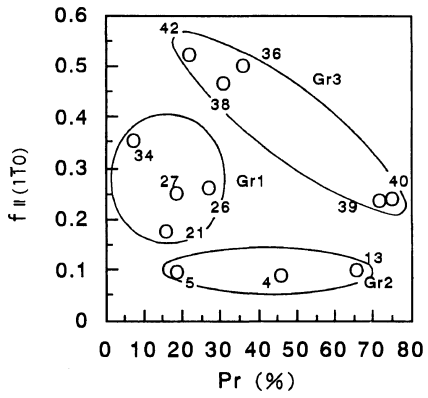

Figure 3. Relation between (1$\bar{1}$0) plane orientation parameter $f_{\parallel(1\bar{1}0)}$ and porosity P_r: Symbols are the same used in Figure 2.

of dehydration power (compression power) of coagulants used for membrane preparations, as discussed on viscose rayon film by Takahashi.[14,15] However, a close inspection reveals that L_t is unexpectedly almost linear decreasing function of P_r if compared at $\chi_c > 30$, but L_t of membranes with low χ_c seems not to be dependent on P_r, giving considerable deviation of L_t at nearly same P_r ($=ca.$ 20%) level (see real ellipsoid in Figure 2a). In addition, the membranes with very low χ_c (<15), which were obtained from organic coagulation systems, constitute one another group (see dotted ellipsoid in Figure 2a) of which L_t is not dependent of P_r. These facts suggest that dehydration power is not sole determinant of swelling anisotropy. As shown in Figure 2b, L_t again unexpectedly tends to increases with an increase in χ_c but scatters strongly at higher χ_c region. On the figure, the circles with top bar mean data points having same porosity P_r($=ca.$ 20%) and the dotted line for the same crystallinity χ_c($=ca.$ 40%). The scattering at higher χ_c region comes in turn from differences in P_r of the corresponding samples, as discussed in Figure 2a. The former fact indicates in part that the membranes with larger amorphous content ($1-\chi_c$) seems to give lower L_t. Figure 2c obviously indicates that L_t is also strongly dependent on (1$\bar{1}$0) crystal plane orientation $f_{\parallel(1\bar{1}0)}$, showing that swelling anisotropy is stronger for higher (1$\bar{1}$0) crystal plane orientation even for the membranes obtained with similar dehydration power or compression imposed during membrane preparation, as shown by straight real line. In addition, as shown in dotted line, membranes obtained by aq. sulfuric acid coagulation systems give another master curve. These facts indicate that plane-orientation mechanism will change depending on coagulation systems.

Therefore, it is important for better understanding of the $f_{\parallel(1\bar{1}0)}$ dependence of L_t to clarify the formation mechanism of (1$\bar{1}$0) plane orientation. Figure 3 shows the relationship between $f_{\parallel(1\bar{1}0)}$ and P_r. Numbers on the data points are χ_c of the samples. It can be clearly recognized that membranes are classified into 3 groups, as shown in three circles in the figure. Group 1 of which $f_{\parallel(1\bar{1}0)}$ is apparently dependent of χ_c with almost constant P_r, is the membranes prepared from cellulose/cuprammonium solution by aq. alkaline coagulation systems. Group 2 of which $f_{\parallel(1\bar{1}0)}$ is independent on P_r with very low χ_c, is the membranes prepared from organic solvent coagulation system. Membranes in Group 3 are prepared from cellulose/cuprammonium solution by aq. acid coagulation systems and their $f_{\parallel(1\bar{1}0)}$ is determined solely by P_r, hence the dehydration power of coagulant. This grouping is essentially the same as discussed for Figure 2a. It should be noted that the cellulose/cuprammonium hydroxide complex is completely destroyed during coagulation for Group 3 and the cellulose/cuprammonium hydroxide complex is altered to another types of complexes during coagulation for Groups 1 and 2, as has been proved in our previous paper.[17] Thus, the changes in complex form of the coagulated cellulose solution might be one of factors controlling the plane-orientation mechanisms of the membranes.

These results and the the fact that water is considered to penetrate into amorphous region preferentially require more detail analysis on amorphous region. For this purpose several membranes with different swelling

anisotropy were chosen for the further analysis. In this connection, the discussion on Group 3 will be reported elsewhere and then omitted here.

Figure 4 shows $\tan\delta$–T curve measured at 10 Hz of the typical membranes grouped above. On the $\tan\delta$–T curves P_r and χ_c of the sample membranes are shown and the relaxation assignments are also shown. According to Manabe *et al.*[13] and Bradley,[14] α_1, α_2, α_{H_2O}, β and γ relaxations are observed at 550—570 K, 410—450 K, 300—330 K, 190—220 K, and 160—175 K, respectively. Group 2 (organic solvent coagulation system) did not exhibit the clear α_1 peak. For Group 1 (alkaline coagulation system) and C10Hs15 (aq. sulfuric acid coagulation in acid coagulation system) in Group 3 showed one overlapped peak for β and γ relaxations. In contrast to this, two clearly separated β and γ peaks were observed for Group 2 and C08Ns10 (aq. ammonium sulfate coagulation in acid coagulation system) in Group 3 but these membranes did not show clear α_1 and α_2 relaxation peaks. Two membranes in Group 3 are characterized by complete destruction of cellulose/cuprammonium hydroxide complex during coagulation but the substance transportation during coagulation is different depending on whether containing ammonium ion in coagulant or not, hence leading to different amorphous structural formation. It is interesting to note that L_t of membrane C08Ns10 is low similar to those for Group 2. Thus, the appearance of β and γ relaxations are essentially influenced by whether coagulation system is organic or aqueous.

All peak temperatures can be more easily detected by loss modulus E''–T curve, shown in Figure 5. Peak temperatures for α_2 and α_{H_2O}, detected from E''–T curves, and their corresponding $\tan\delta_{max}$ are listed in Table II. The peak temperatures for the β and γ relaxations and their $\tan\delta$ values are also listed in Table II. Here, due to the complexity of α peak appearance, we adopted a maximum loss modulus E'' peak as α_2 peak, a higher temperature E'' peak as α_{H_2O}, in their temperature region. The adoption of the present α_2 peak might be suitable for discussion on dimensional stability (swelling behavior) against water since this relaxation has been attributed to the micro Brownian motion of molecular chain having different strength of intra- and inter-molecular hydrogen bonds.[13]

Regarding β relaxation, Manabe *et al.*[27] very recently reported that the relaxation region is composed of two components at -60 and -90°C of which latter peak disappears by treatment of cellulose with organic solvent. Then, we also examined the magnified $\tan\delta$–T curves in lower temperature region (see Figure 6) more carefully. Obviously, the membranes prepared by aque-

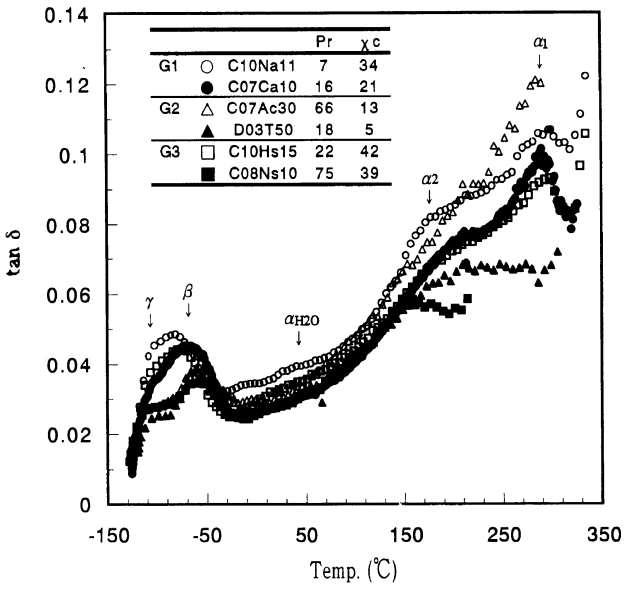

Figure 4. Loss tangent $\tan\delta$–temperature T curves for typical membranes in the T range -150 to 350°C: ○, C10Na11; ●, C10Hs15; △, C07Ac30; ▲, D03T50; □, C10Hs15; ■, C08Ns10.

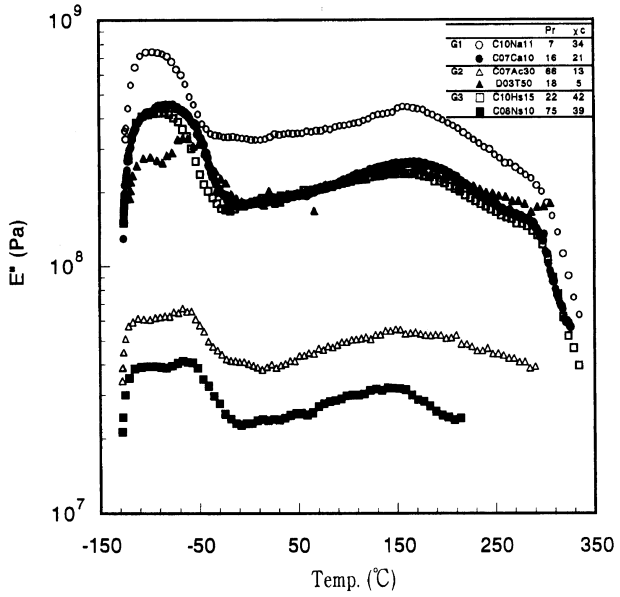

Figure 5. Loss modulus E''–temperature T curves for typical membranes in the T range -150 to 350°C: Symbols are the same as used in Figure 4.

Table II. Super-molecular parameters of regenerated cellulose membranes

Sample	Mechanical relaxations								Remarks
	γ		β		α_{H_2O}		α_2		
	T_{max}/K	$\tan\delta_{max}$	T_{max}/K	$\tan\delta_{max}$	T_{max}/K	$\tan\delta_{max}$	T_{max}/K	$\tan\delta_{max}$	L_t
C10Na11	163	0.042	191	0.049	300	0.038	430	0.075	1.97
C10Hs15	161	0.034	198	0.044	305	0.034	442	0.066	1.99
C08Ns10	163	0.027	217	0.038	323	0.032	413	0.055	1.21
C07Ac30	167	0.028	215	0.038	316	0.034	421	0.067	1.61
C07Ca10	169	0.035	204	0.046	313	0.031	432	0.064	1.71
D03T50	175	0.025	213	0.039	328	0.034	428	0.056	1.58

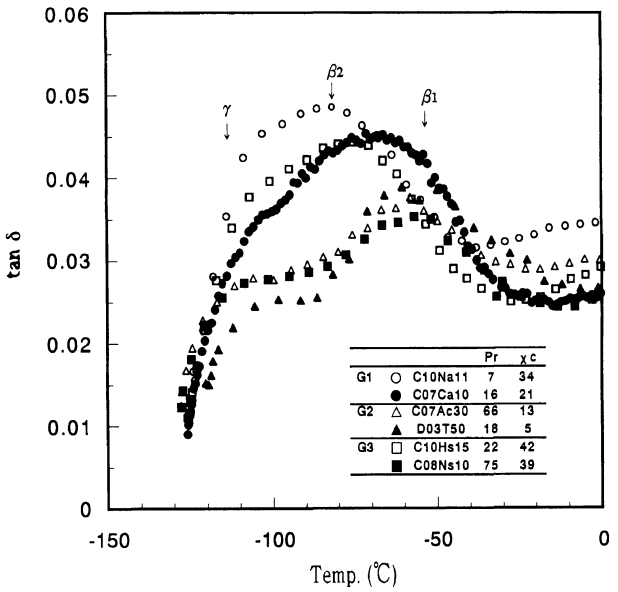

Figure 6. Magnified loss tangent tan δ–temperature T curves for typical membranes in β and γ relaxation region: Symbols are the same as used in Figure 4.

ous coagulation systems exhibit one major peak (β_2 at *ca.* -80°C) with a shoulder at higher temperature side and the membranes prepared by organic coagulation systems have one major peak (β_1 at *ca.* -60°C) with at least 2 shoulders at lower temperature side in β relaxation region. Major peaks for both membrane groups are the same as those used for analyzing in Table II. The former major peak seems apparently to disappear for the membrane prepared with organic solvent coagulation system (Group 2), which is well corresponding to Manabe *et al.*s' observation. β_2 relaxation should relate to the amorphous region corresponding to the structure formed by dehydration of water during membrane formation and β_1 relaxation might relate to the so-called hydrophobic interaction. Note that the membrane C08Ns10 in Group 3 which is prepared from cellulose in cuprammonium hydroxide solution with ammonium sulfate as coagulant shows similar tan δ–T curves to those for membranes prepared by organic solvent coagulation system. This means that the above discussion is not always applicable or that even for the aqueous coagulation system in the regenerated cellulose membrane formation from its cuprammonium cellulose solution an excess amount of ammonium ion in the system might behave like as organic compound. Thus, C08Ns10 should be dealt as an exception. T_{max} and corresponding tan δ_{max} for β_1 and β_2 evaluated from Figure 6 are collected in Table III. Note that T_{max} and tan δ_{max} for the main peak collected in Table II on the whole give the characteristic information of the membranes and therefore the values in Table II will be employed in further analysis.

Figure 7 shows storage modulus E'–T curves, indicating in general that the larger E' resulted for the membranes with lower P_r because E' is estimated for unit area. Then, the reduced E' values for α_2, α_{H_2O}, β and γ relaxations, reestimated per unit weight/unit area using P_r values, and are also collected in Table II.

Some of the parameters collected in Table II are

Table III. Mechanical relaxations of β absorption for regenerated cellulose membranes

Sample	β_2		β_1		tan $\delta_{max\beta_2}$/ tan $\delta_{max\beta_1}$
	T_{max}/K	tan δ_{max}	T_{max}/K	tan δ_{max}	
C10Na11	191.1	0.0485	204.8	0.0450	1.078
C10Hs15	197.9	0.0442	211.1	0.0400	1.105
C08Ns10	206.2	0.0341	216.2	0.0350	0.974
C07Ac30	206.2	0.0360	215.0	0.0380	0.952
C07Ca10	201.4	0.0456	218.7	0.0430	1.060
D03T50	202.1	0.0360	212.4	0.0390	0.923

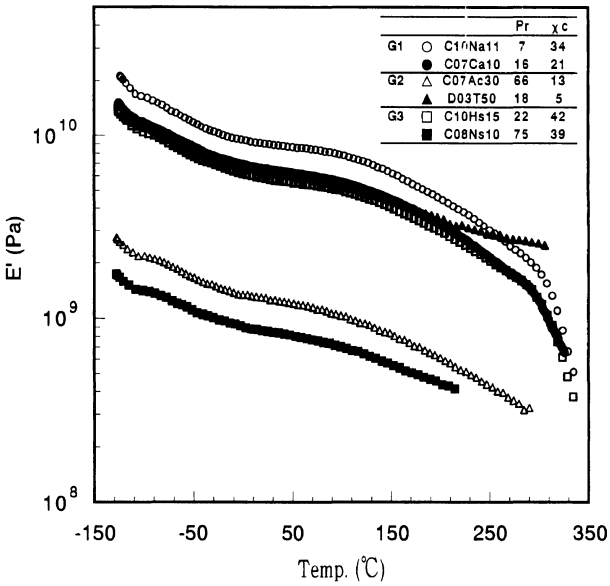

Figure 7. Storage modulus E'–temperature T curves for typical membranes in the T range -150 to 350°C: Symbols are the same as used in Figure 4.

tentatively plotted against swelling anisotropy parameter L_t in Figures 8A—C (a, α_2; b, α_{H_2O}; c, β; d, γ relaxations). Open circles mean the data points for Group 1, closed circles for Group 2 and circles with horizontal bar for Group 3. Data points with similar P_r(=*ca.* 20%) are marked with top bar and the numbers denote χ_c. It is one of purpose to seek for the parameter explaining approximately the swelling anisotropy. Lower $T_{max}\alpha_{H_2O}$, $T_{max}\beta$, and $T_{max}\gamma$ resulted approximately in larger L_t although Group 3 seems to give another master curve for α_{H_2O} and γ relaxations. The reverse tendency is observed for $T_{max}\alpha_2$. These results suggest that α_2 and other relaxations contain mutually cooperative or alternative information, respectively. In other words, α_{H_2O}, β, and γ relaxations give similar structural information (segmental motion) in part. The fact that lower $T_{max}\alpha_{H_2O}$ gives larger L_t might relate to the existence of amorphous structure with molecular chains relatively easily moved by water but $T_{max}\alpha_{H_2O}$ does not give direct causal sequence for swelling anisotropy unless its mechanical relaxation mechanism is clarified. Note that the same holds for all other relaxations. The result for α_2 indicates unexpectedly that the amorphous region with stronger inter- and intra-molecular hydrogen bonds causes larger swelling anisotropy. $T_{max}\alpha_2$ easily moves down to far lower temperature by water absorption, as pointed out by Manabe *et al.*,[13] suggesting that α_2 relaxation is

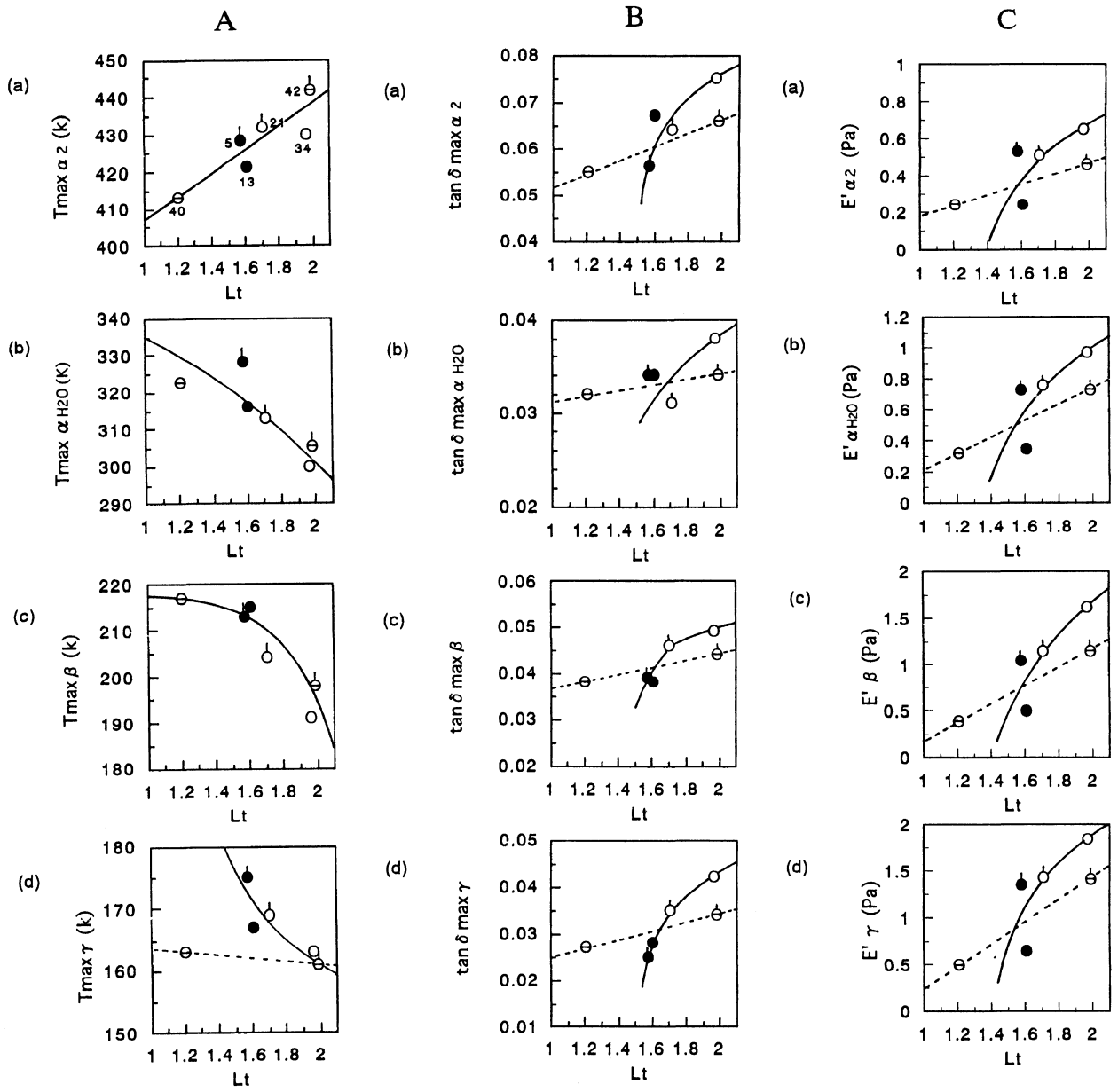

Figure 8. Dependence of swelling anisotropy parameter L_t on amorphous parameters (A, T_{max}; B, $\tan\delta_{max}$; C, E'; (a), α_2; (b), α_{H_2O}; (c), β; (d), γ relaxations).

associated with segmental motion based on the disruption of intermolecular interaction (that is, mainly intermolecular hydrogen bond). However, this fact alone could not explain the above result. One possible explanation is that $T_{max}\alpha_2$ is a measure for molecular packing in main amorphous region, from which anisotropic structural integration induced by water grows. Such anisotropic structural integration accompanies the swelling anisotropy and of course water is retained in such anisotropic structural integration. In this regard, it should be noted that L_t is a result after water absorption and all the above amorphous parameters are for practically dried membranes. Figure 7B shows that naturally the larger $\tan\delta_{max}$ values for all relaxations give the larger L_t on the whole, indicating that larger amorphous content results in higher swelling anisotropy as a result. Note that $\tan\delta_{max}$ values are the index of amorphous content and should be related to amount of the absorbed water not to directly its swelling anisotropy. Clearly, $\tan\delta_{max}$–L_t relation for Group 3 is somewhat different from other groups.

The reduced E' corresponding to each relaxation for membranes with constant P_r does not influence L_t, but larger E' tends to give larger L_t on the whole, as shown in Figure 7C. Here again, Group 3 constitutes one distinct group. Although no stretching procedure was applied for the membrane preparation the stretching by self contraction during membrane preparation is possible. Then, the E' value might be composed of the contribution from crystalline parts and from strong hydrogen bonding part (or molecular oriented part) in amorphous region. Crystalline part is of course composed of molecular chains with well developed hydrogen bonding. Therefore, the present results indicate that membrane with strong hydrogen bonding or relatively highly oriented part gives larger swelling anisotropy. This is a supplement for the discussion given for $T_{max}\alpha_2$–L_t relation above.

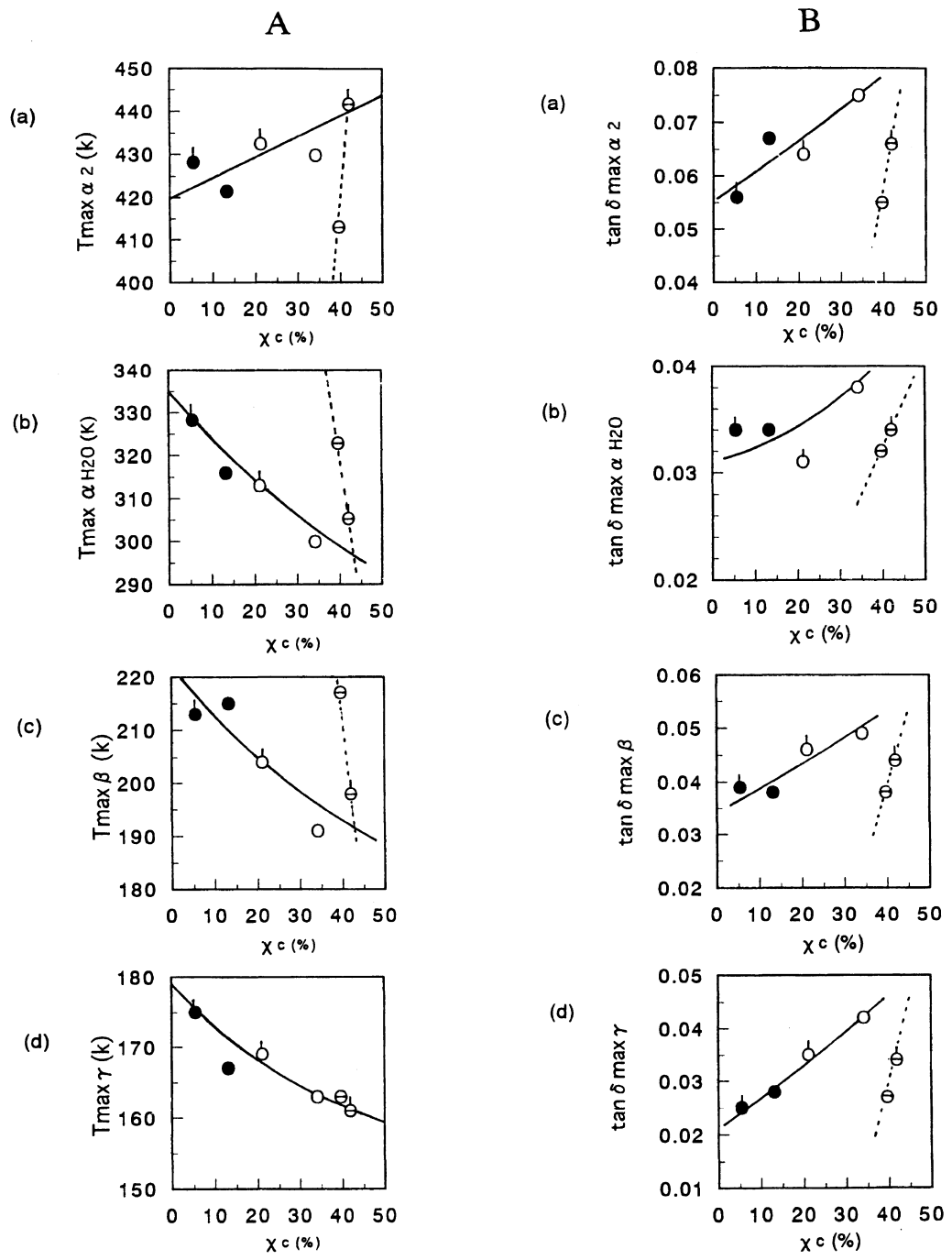

Figure 9. Dependence of amorphous parameters (A, T_{max}; B, $\tan\delta_{max}$) on crystallinity χ_c; (a), α_2; (b), α_{H_2O}; (c), β; (d), γ relaxations).

Thus, most of the amorphous parameters could describe the swelling anisotropy except Group 3 and on the whole, $T_{max}\beta$ might be most reliable, judging from Figure 8. As was pointed out before, it is needed to clarify the mechanical relaxation mechanism for each relaxation peak associated with other structural parameters in order to obtain more direct causal relation to the swelling anisotropy.

Then amorphous parameters (T_{max}, $\tan\delta_{max}$) are plotted against χ_c and $f_{\|(1\bar{1}0)}$ in Figures 9A, B, and 10A, B. As will be expected from Figure 2 all the amorphous parameters as functions of χ_c and $f_{\|(1\bar{1}0)}$ are quite similar as well as their L_t dependence. But, note that the positive linear relation between χ_c and $f_{\|(1\bar{1}0)}$ is not always required. Groups 1 and 2, and Group 3 constitute each master curve for α_2, α_{H_2O}, and β relaxations, respectively. For $T_{max}\gamma$ relaxation the relations seem to give one master curve, irrespective of samples, indicating that γ relaxation seems to be an inherent parameter associated with crystallinity and its plane orientation. Larger χ_c or $f_{\|(1\bar{1}0)}$ gives larger $T_{max}\alpha_2$ and lower T_{max} for other relaxations (α_{H_2O}, β, and γ) and $\tan\delta_{max}$ for all relaxations increases with an increase in χ_c or $f_{\|(1\bar{1}0)}$. Note that amorphous parameters for β_1 and β_2 show naturally similar χ_c- and $f_{\|(1\bar{1}0)}$-dependencies to that of β although not shown here.

Since larger χ_c indicates the stronger molecular packing (hence stronger inter-molecular hydrogen bond) also in amorphous region in general, main micro Brownian motion associated with intermolecular hydrogen bond

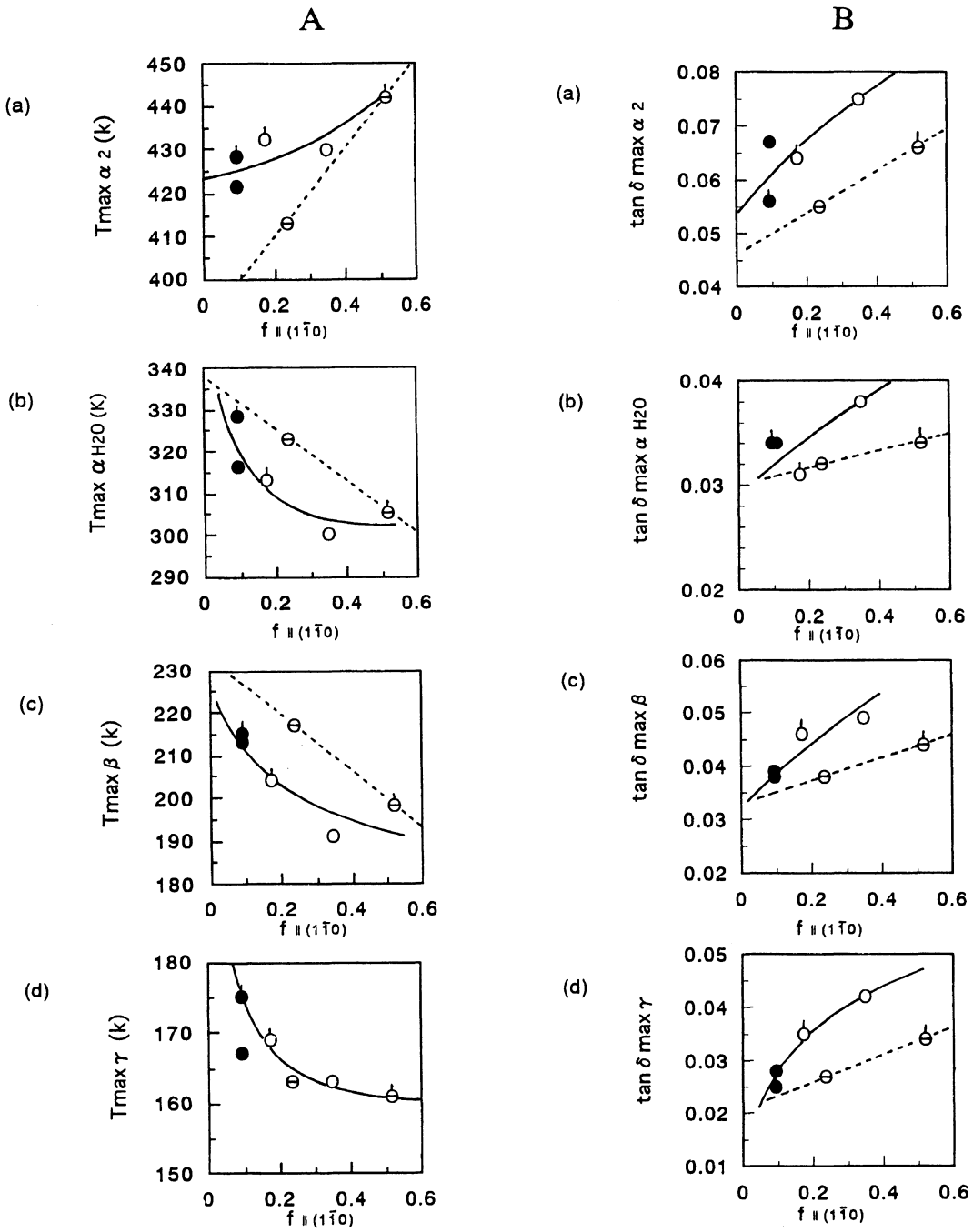

Figure 10. Dependence of amorphous parameters (A, T_{max}; B, $\tan\delta_{max}$) on ($1\bar{1}0$) plane orientation parameter $f_{\parallel(1\bar{1}0)}$; (a), α_2; (b), α_{H_2O}; (c), β; (d), γ relaxations).

above glass transition temperature (T_g) should be hard to occur, then it is reasonable that larger χ_c results in higher $T_{max}\alpha_2$. In other words, higher $T_{max}\alpha_2$ is the basis to give higher crystallinity during coagulation as a result by considering that crystallization takes place in almost complete amorphous region by for example, nucleation. The characteristic structure that larger χ_c gives larger $\tan\delta_{max}$ for α_2 relaxation will be possible by excluding some of molecular chains existed between some ordered region to amorphous region when the ordered region is integrated into crystalline region. This is reasonable because the molecular aggregate are not always composed of simple crystal and amorphous components. This explanation will also hold for other relaxations. However, regarding their T_{max} the situation is somewhat different from α_2 relaxation because other relaxations are always active below T_g or room temperature due to their local segmental motions. When a part of amorphous region is integrated into crystalline region (that is, an increase in χ_c), more liable or mobile parts corresponding to such local segmental motions will remain on the whole in the remaining or newly excluded amorphous region, exhibiting lower T_{max}. This explanation is far from the true answer but is one of possibilities.

Similar discussion could hold for $f_{\parallel(1\bar{1}0)}$ dependence of T_{max} and $\tan\delta_{max}$ for all relaxations. The higher $f_{\parallel(1\bar{1}0)}$ means that intermolecular hydrogen bonds between ($1\bar{1}0$) sheets (that is, out-of-phase interaction) is more oriented to the membrane thickness direction. This direction is the direction of substance transportation

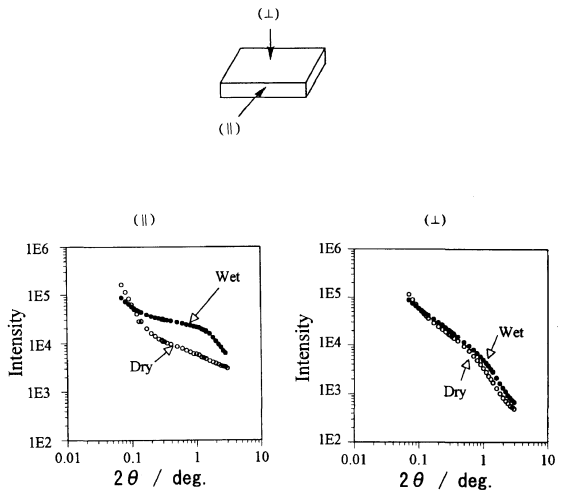

Figure 11. Small angle X-ray diffraction patterns of a cellulose membrane taken at parallel (∥) and perpendicular (⊥) directions: ○, at dry state; ●, at wet state.

direction during coagulation and drying in membrane formation. If the substance transported is water the water transportation might align the intermolecular hydrogen bonds on polymer chains to the thickness direction, depending on its transportation speed and the stability of the coagulated cellulose complex. It is natural to think that this coagulation mechanism will be applicable to amorphous region. Therefore, higher $f_{\parallel(1\bar{1}0)}$ is associated with microscopical molecular aggregate having relatively strong intermolecular hydrogen bond, leading to higher $T_{max}\alpha_2$. However, T_{max} for other relaxations associated with local segmental motions decreases by higher order integration of molecular chains in $(1\bar{1}0)$ sheet-like orientation, as discussed before. This means that more ordered such sheet-like structure is not simply assumed in amorphous region accompanied with higher $f_{\parallel(1\bar{1}0)}$. In other words, larger the content of ordered region, larger the strain in the remaining if external force is not applied during membrane formation. This is indirectly affirmed by $T_{max}\gamma$–$f_{\parallel(1\bar{1}0)}$ relation. If more ordered such sheet-like structure is simply assumed in amorphous region, then rotational motion of C_6 around C_5–C_6 axis should be restricted with an increase in $f_{\parallel(1\bar{1}0)}$, leading to higher temperature shift of T_{max} but the experimental results are reversed.

β_2 relaxation, which apparently disappears by organic solvent coagulation, might relate to local segmental motion associated with existence of water rather to the out-of phase direction in $(1\bar{1}0)$ plane sheet-like amorphous structure. β_1 relaxation, which survives by organic solvent coagulation system, might relate to the in-phase segmental motion, that is, segmental motion to van der Waals direction.

Thus, the swelling anisotropy is the phenomenon that arises from water penetration to more mobile parts (giving lower T_{max} for γ, β, and α_{H_2O}), plasticizing molecular chains and integrating some of them on more ordered original $(1\bar{1}0)$ planes according its direction ($f_{\parallel(1\bar{1}0)}$) or simply displacing original components with higher plane orientations to thickness direction. This mechanism will be affirmed from Figure 11 where shows the results of typical small angle X-ray analysis for a regenerated membrane in dry and wet states. Obviously, a distinct increase in the diffraction intensity is seen for $(1\bar{1}0)$ plane, compared with that for (200) plane. This means that the swelling anisotropy observed in the present study accompanies the anisotropical change in long periodicity between elemental crystal planes from 7 nm to 11 nm (widening of $(1\bar{1}0)$ plane).

In conclusion, the swelling anisotropy observed for various regenerated cellulose membranes is the phenomenon relating to the degree of the out-of-phase hydrogen bonding (intermolecular hydrogen bonding) against in-phase-interaction (so-called hydrophobic interaction), which are characterized especially by α_{H_2O}, β, and γ relaxations.

REFERENCES

1. K. Kamide, K. Okajima, T. Matsui, and K. Kowsaka, *Polym. J.*, **16**, 857 (1984).
2. T. Yamashiki, T. Matsui, M. Saito, K. Okajima, and K. Kamide, *Br. Polym. J.*, **22**, 73 (1990).
3. T. Yamashiki, T. Matsui, M. Saito, K. Okajima, and K. Kamide, *Br. Polym. J.*, **22**, 121 (1990).
4. K. Kamide, K. Okajima, and K. Kowsaka, *Polym. J.*, **24**, 71 (1992).
5. T. Yamashiki, T. Matsui, K. Kowsaka, M. Saito, K. Okajima, and K. Kamide, *J. Appl. Polym. Sci.*, **44**, 691 (1992).
6. T. Yamane, M. Saito, and K. Okajima, submitted to *Sen-i Gakkaishi*.
7. M. Tomokiyo, H. Yamazaki, F. Ise, T. Koizumi, M. Ohtsuka, and K. Okajima, *Polym. J.*, submitted.
8. T. Koizumi, H. Ono, M. Tomokiyo, and K. Okajima, submitted to *Polym. J.*
9. T. Koizumi and K. Okajima, submitted to *J. Appl. Phys.*
10. I. Sakurada and S. Okamura, *Kougyou Kagaku Zatttusi*, **40**, 909 (1937).
11. P. H. Hermans, *J. Polym. Sci.*, **4**, 145 (1949).
12. J. Hayashi, J. Masuda, and Y. Watanabe, *Nippon Kagaku Kaishi*, **5**, 948 (1974).
13. S. Manabe, M. Iwata, and K. Kamide, *Polym. J.*, **18**, 1 (1986).
14. S. A. Bradley and S. H. Carr, *J. Polym. Sci., Polym. Phys. Ed.*, **14**, 111 (1976).
15. T. Takahashi, *Sen-i Gakkaishi*, **25**, 80 (1969).
16. T. Takahashi, *Sen-i Gakkaishi*, **25**, 122 (1969).
17. M. Inamoto, I. Miyamoto, T. Hongo, M. Iwata, and K. Okajima, submitted to *Polym. J.*
18. K. H. Illers, *Makromol. Chem.*, **38**, 168 (1960).
19. D. C. Prevorsek, R. H. Burler, and J. A. Reimschuesel, *J. Polym. Sci., A-2*, **9**, 867 (1971).
20. K. Schmieder and K. Wolf, *Kolloid-Z.*, **134**, 149 (1953).
21. B. A. Dunnel and S. J. W. Price, *J. Polym. Sci.*, **18**, 305 (1955).
22. W. Gibbson, L. Spencer, and R. McCall, *J. Chem. Soc.*, **117**, 479 (1920).
23. W. Brown and R. Wikstrom, *Eur. Polym. J.*, **1**, 1 (1965).
24. A. F. Turbak, "Proceedings 1983 International Dissolving and Speciality Pulps Conference," Tappi, Atlanta, U.S.A., 1983, p 105.
25. L. Segal, J. J. Creely, A. E. Martin, Jr., and C. M. Conrad, *Text. Res. J.*, **786** (1959).
26. Y. Shimaya, M. Hattori, and M. Saito, submitted to *Polym. J.*
27. S. Manabe and R. Fujioka, submitted to *Polym. J.*